J. E. Bobrow

J. M. McCarthy

V. K. Chu

Department of Mechanical Engineering,
University of California, Irvine,
Irvine, California 92717

Time-Optimal Control of Two Robots Holding the Same Workpiece

An algorithm is given which minimizes the time for two robots holding the same workpiece to move along a given path. The unique feature of these systems is that they have more actuators than degrees of freedom. The method can be applied to any constrained robot system, including the case where one robot arm moves in contact with a surface. In addition to finding the optimum torque histories, the algorithm determines the optimum contact force between the each robot and the workpiece throughout the motion. Constraints on these internal forces are easily introduced into the algorithm.

1 Introduction

One approach for finding time-optimal trajectories for open and closed chained robots is to assume the path is unconstrained, and use Pontryagin's maximum principle to derive the necessary conditions for optimality. Researchers have developed specialized numerical methods to solve the equations which satisfy the optimality conditions (see Kahn and Roth, 1971; Meier and Bryson, 1987; and Chen and Desrochers, 1988). These methods are usually difficult to use in practical situations where there are obstacles in the workspace.

Another approach is to assume that the path is given, either in joint space or Cartesian space, but the motion in time along it is unknown. In this case, the time-optimal velocity profile for the given path can be found using an algorithm such as in Bobrow et al. (1985) or Shin and McKay (1985). Besides numerical efficiency, advantages to this approach over the maximum principle are that motions which avoid obstacles can be specified, and that paths can be varied in search for an optimum using parameter optimization algorithms (Rajan, 1985; Gilbert and Johnson, 1985; Shiller and Dubowsky, 1988; Bobrow, 1988).

This paper generalizes the work in Bobrow et al. (1985) for open-chained robots to the case of closed-chained, or constrained robots. Cases of such systems include robots cooperating to perform an assembly task, grasping, walking, and one robot moving in contact with a constraint surface. The systems are all redundantly actuated, meaning that there are more actuators than degrees of freedom. Previous research on these systems has been on balancing the load among the actuators, (see for example Kreutz and Lokshin, 1988; Zheng and Luh, 1988) and to control the internal forces acting on the object, (Walker et al., 1989). The case of controlling motion of one robot in contact with a surface is considered by Mills and Goldenberg (1989) and by McClamroch and Huang (1988), where the time-optimal control problem is formulated.

The main contributions of this research are: 1) A new algorithm is developed which produces the time-optimal trajectory along a specified path for constrained robot systems, including the optimal open-loop actuator inputs as functions of time; 2) A straightforward method is given to solve the problem when bounds are specified on *internal forces* as well as the actuators, and; 3) It is shown that at any instant during an optimal motion, at least $m+p+1-n$ actuators or internal forces will be saturated, where m is the number of independent constraint equations, n is the number of coordinates used to describe the system, and p is the number of actuators.

2 Dynamics of Cooperating Robots

In this section the equations of motion for the closed chain formed by a pair of cooperating manipulators are derived, assuming that the end-effector of each robot rigidly holds the workpiece. The combination of these end-effectors and the workpiece is viewed as a single moving rigid body. The form of the equations obtained is the same as any constrained system, so the analysis applies to one robot arm moving along a surface, and other applications.

Let q_1 define the position of one robot arm, q_2 the other arm, and q_3 the position of the workpiece. In order to have a concrete example, refer to the closed chain shown in Fig. 1. In this case, $q_1=(\theta_1, \phi_1)^T$, $q_2=(\theta_2, \phi_2)^T$, and $q_3=(x, y, \alpha)^T$. The Cartesian position of some point p on the workpiece can be written as a function of the workpiece coordinates q_3 alone, $p=p(q_3)$, or as a function of the end-effector position of either arm and the orientation of the workpiece, i.e.,

$$p(q_3)=\tilde{p}(q_1, q_3), \tag{1}$$

and

$$p(q_3)=\hat{p}(q_2, q_3), \tag{2}$$

Contributed by the Dynamic Systems and Control Division for publication in the JOURNAL OF DYNAMIC SYSTEMS, MEASUREMENT, AND CONTROL. Manuscript received by the Dynamic Systems and Control Division April 19, 1990; revised manuscript received August 28, 1992. Associate Technical Editor: R. Horowitz.

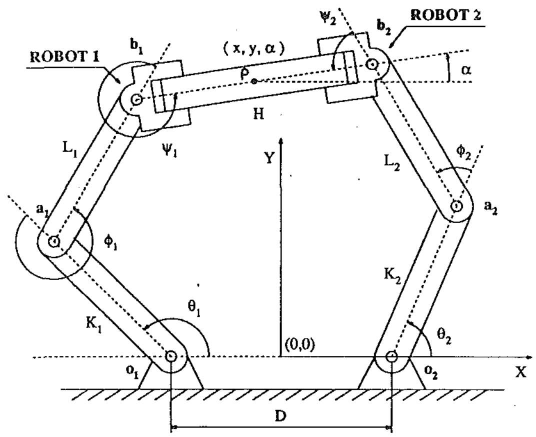

Fig. 1 A pair of 3R planar robots holding the same workpiece

The closure Eqs. (1) and (2) represent m holonomic constraints, where $m=4$ for planar problems, and $m=6$ in general. Note that this approach does not require constraint equations relating the orientation of the workpiece to the orientation of each end-effector since the end-effector coordinates are not included in q_1 or q_2, i.e., they are determined from q_3 (this can always be done for wrist-partitioned robots). The number of independent degrees of freedom is $n-m$, where n is the total number of coordinates used to define the position of the complete system. For the planar example in Fig. 1, $n=7$, with two degrees of freedom for each arm, and three for the workpiece.

Differentiating (1) and (2) with respect to time gives the nonholonomic form of the closure constraints

$$J_3\dot{q}_3=\tilde{J}_1\dot{q}_1+\tilde{J}_3\dot{q}_3, \tag{3}$$

and

$$J_3\dot{q}_3=\hat{J}_2\dot{q}_2+\hat{J}_3\dot{q}_3, \tag{4}$$

where J_3 is the matrix of partial derivatives (Jacobian) of $p(q_3)$ with respect to q_3, and $\tilde{J}_1$ the Jacobian of $\tilde{p}$ with respect to q_1. Similar definitions hold for $\tilde{J}_3$, $\hat{J}_2$, and $\hat{J}_3$.

The equations of motion of the three sub-systems have the form:

$$M_1(q_1)\ddot{q}_1+h_1(q_1,\dot{q}_1)=u_2+c_1, \tag{5}$$

$$M_2(q_2)\ddot{q}_2+h_2(q_2,\dot{q}_2)=u_2+c_2, \tag{6}$$

$$M_3(q_3)\ddot{q}_3+h_3(q_3,\dot{q}_3)=u_3+c_3, \tag{7}$$

where M_i, h_i are the corresponding mass matrix, Coriolis and gravity terms, respectively, and u_i are the generalized forces due to the actuators for each system. The vectors c_i represent the generalized forces due to interaction of the three systems. To derive these equations of motion, each of the three systems are first considered to be independently acting, unconstrained systems so that the standard form of Lagrange's Equations may be applied to obtain the M_i and h_i with the interaction forces $c_i=0$. The following approach may then be used to obtain the interaction or constraint forces c_i.

In order to relate the constraint forces c_i to the dynamics of the system, use the fact that the constraints do no work (do not absorb power). Hence, defining $c^T=(c_1^T,\ c_2^T,\ c_3^T)$ and $q^T=(q_1^T,\ q_2^T,\ q_3^T)$, we have

$$c^T\dot{q}=0, \tag{8}$$

for all admissible velocities $\dot{q}$. If there were no constraints on the individual systems, as in the open-chained case, the velocities $\dot{q}_i$ of each system could vary arbitrarily and (8) shows that the forces of interaction c_i would be zero (i.e., in general, given x, $y\in\Re^n$, if $x^Ty=0$ for all y then $x=0$).

The joint velocities $\dot{q}$ must also satisfy the constraints (3) and (4), or combining them,

$$\Phi(q)\dot{q}=0, \tag{9}$$

where

$$\Phi(q)=\begin{bmatrix}\tilde{J}_1 & 0 & \tilde{J}_3-J_3\\ 0 & \hat{J}_2 & \hat{J}_3-J_3\end{bmatrix}.$$

Note that nonholonomic constraints can also be written in the same form as (9), hence the following derivation also applies to systems with nonholonomic constraints.

For every admissible velocity vector $\dot{q}$ satisfying (9), we have a vector of constraints c which satisfies (8). Equation (9) shows that $\dot{q}$ is in the null space of $\Phi(q)$, and (8) shows that c is orthogonal to $\dot{q}$, thus c is in the orthogonal complement of the null space of $\Phi(q)$. This means that c is in the range of $\Phi(q)^T$ or that there exists a vector $\lambda\neq 0$ such that

$$c=\Phi(q)^T\lambda. \tag{10}$$

Note that λ represents internal forces of the closed chain system. The coupled equations of motion for the system become

$$M(q)\ddot{q}+h(q,\dot{q})=u+\Phi(q)^T\lambda, \tag{11}$$

where

$$M(q)=\begin{bmatrix}M_1 & 0 & 0\\ 0 & M_2 & 0\\ 0 & 0 & M_3\end{bmatrix},$$

$$h(q,\ \dot{q})=\begin{pmatrix}h_1\\ h_2\\ h_3\end{pmatrix},\ \text{and}\ u=\begin{pmatrix}u_1\\ u_2\\ u_3\end{pmatrix}.$$

In general (see the Appendix), the generalized forces u are related to the actuator torques $\tau\in R^p$ by a matrix transformation of the form

$$u=B\tau, \tag{12}$$

where B is an $n\times p$ matrix with p usually less than n.

3 Optimal Motion Along a Specified Path

3.1 Path Parametrization. In order to find the time-optimal motion for a given path, the motion of all the degrees of freedom must be specified as functions of some scalar path parameter s. In general, the number of degrees of freedom is $n-m$, where n is the total number of joint coordinates used and m is the number of constraints for the system. Hence, the motion of $n-m$ joint displacements must be given in order to uniquely specify the path.

In the example given in this paper, we parameterized the motion of the workpiece as

$$q_3=q_3(s),\quad s\in[0,\ 1], \tag{13}$$

with $q_3(0)=q_{3o}$ the start position, and $q_3(1)=q_{3f}$ the final position. In this case, the remaining degrees of freedom q_1 and q_2 may be determined for each position s of the workpiece from the inverse kinematic solution for each arm.

To determine the time-optimal motion, the optimal solution $s(t)$, $t\in[0,\ t_{\text{final}}]$ must be found. To accomplish this, the velocity and acceleration of each joint are needed as a function of s, $\dot{s}$, and $\ddot{s}$. Since the motion of the workpiece is specified explicitly, (13) is differentiated twice to obtain

$$\dot{q}_3=\frac{dq_3}{ds}\dot{s} \tag{14}$$

$$\ddot{q}_3=\frac{d^2q_3}{ds^2}\dot{s}^2+\frac{dq_3}{ds}s\ddot{s} \tag{15}$$

The velocities $\dot{q}_1$ and $\dot{q}_2$ can then be found knowing $\dot{q}_3(s,\ \dot{s})$ using (3) and (4). Similarly, the accelerations $\ddot{q}_1$ and $\ddot{q}_2$ can be found knowing $\ddot{q}_3$ from (15) by differentiating (9) with respect to time and solving the two matrix equations for the two unknowns, $\ddot{q}_1$ and $\ddot{q}_2$. The final form of the joint acceleration vector is

$$\ddot{q}=a(s,\ \dot{s})\ddot{s}+b(s,\ \dot{s}). \tag{16}$$

Substituting (16) and (12) into the equations of motion (11), a set of n second order differential equations are obtained in terms of the scalar path parameter $s(t)$:

$$c_1(s,\ \dot{s})\ddot{s}+c_2(s,\ \dot{s})=B\tau+\Phi^T\lambda, \tag{17}$$

where $c_1(s,\ \dot{s})=Ma$, and $c_2(s,\ \dot{s})=Mb+h$. Note that for any motion $s(t)$, $\dot{s}(t)$, $\ddot{s}(t)$, (17) represents n equations with $p+m$ unknown actuator inputs $\tau(t)$, and constraint forces $\lambda(t)$. If $p>n-m$, there are more actuators than degrees of freedom and there is no unique solution for $\tau(t)$ and $\lambda(t)$. However, because the actuator inputs are bounded, we can use this redundancy to decrease the motion time for a specified path as follows.

3.2 Time Optimization. The time required to traverse a given path is

$$t_f=\int_0^1 \frac{ds}{\dot{s}}, \tag{18}$$

and it is the time t_f which we seek to minimize. The time-optimal control problem is to find $s(t)$ that minimizes t_f subject to the equations of motion (17), actuator limitations

$$\tau^{\min}\le\tau\le\tau^{\max} \tag{19}$$

and possible limitations on the forces applied to the workpiece

$$\lambda^{\min}\le\lambda\le\lambda^{\max}. \tag{20}$$

To find the optimal $s(t)$, let the scalar path acceleration be the control variable for the transformed problem: Find $\hat{u}(t)$ which minimizes t_f and drives the system

$$\ddot{s}=\hat{u} \tag{21}$$

from $s(0)=\dot{s}(0)=0$ to $s(t_f)=1$, $\dot{s}(t_f)=0$ subject to $f(s,\ \dot{s})\le\hat{u}\le g(s,\ \dot{s})$.

For any position and velocity along the path $(s,\ \dot{s})$, the term $f(s,\ \dot{s})$ is the minimum possible acceleration, and $g(s,\ \dot{s})$ is the maximum possible acceleration. To find these values, note that

$$f(s,\ \dot{s})=\text{minimum }\{\ddot{s}\} \tag{22}$$

subject to: (17), (19), and (20). Because all coefficients in the equations of motion (17) are known for any position and velocity $(s,\ \dot{s})$, the unknown $\ddot{s}$, corresponding joint actuator inputs τ, and internal forces λ all appear *linearly* in (17). Hence, $f(s,\ \dot{s})$ can be computed efficiently as the solution to a standard linear programming problem using an algorithm such as the Simplex Method (Thie, 1979).

When the motion of the system is not along a singular arc (see Shiller, 1990), the time optimal solution to the transformed problem is bang-bang in the control $\hat{u}$. That is, at any instant, $\hat{u}=f(s,\ \dot{s})$ or $\hat{u}=g(s,\ \dot{s})$. In the case where there is only one switch from acceleration along the path to deceleration, the switching time is found by setting $\hat{u}=g(s,\ \dot{s})$ and integrating (21) forward in time from the initial position $(s,\ \dot{s})=(0,\ 0)$, and then integrating (21) backwards in time with $\hat{u}=f(s,\ \dot{s})$ from the final position $(s,\ \dot{s})=(1,\ 0)$. The switching point occurs at the intersection of the two trajectories. The details of the algorithm for this case and the case of multiple switching times are identical to that in Bobrow et al. (1985), except that the functions $f(s,\ \dot{s})$ and $g(s,\ \dot{s})$ must now be found by solving a linear programming problem.

From the above discussion it is seen that the main computational burden is the numerical integration of a nonlinear second order ordinary differential equation plus the determination of switching points. For the numerical integration, we used a fifth order Runge-Kutta routine (IMSL routine DVERK), which has a user specified integration tolerance. At each integration step the solution to the linear programming problem is needed to determine $f(s,\ \dot{s})$ and $g(s,\ \dot{s})$. If we assume that this computation is done in constant time, then the time for computation of the entire solution depends linearly on the number of integration steps. Hence, for a fixed numerical integration tolerance, the computation time grows linearly with the path traversal time. Switching points are also computed in approximately constant time, so the total computation time has the form $t_{\text{comp}}=a_1t_f+a_2N_{ts}$, where t_f is the path traversal time, N_{ts} is the number of switches between acceleration and deceleration, and a_1, a_2 are constants.

3.3 Number of Saturated Actuators or Internal Forces. The solution to the above linear programming problem yields, at each instant; (a) the maximum or minimum acceleration $\ddot{s}$, (b) the m corresponding internal forces λ, and (c) the p joint actuator torques or forces τ. Hence, the number of unknowns are $m+p+1$, and there are $n+p+m$ possible linear constraint equations active at each instant, defined by (17), (19), and (20).

For a bounded solution to the LP problem, the same number of constraint equations must be active as the number of unknowns. The total number of possible actuators τ_i or internal forces λ_i saturated at any instant is then at least $m+p+1-n$ which is the difference between the number of unknowns and number of constraints in (17). It is at least this many because if fewer than n constraints in (17) are active, then more actuators or internal force constraints must become active. A more rigorous explanation of this phenomenon is given in McCarthy et al. (1992).

4 Numerical Examples

As an example application of the algorithm presented in this paper, the workpiece is moved from the start position to the end position shown in Fig. 2 along different paths. Five uniform cubic B-spline control points (Schumaker, 1981) are used to define the path of the workpiece shown in Fig. 2(a), and Fig. 3(a). The difference in the two paths results in a change in path traversal time, with the time for Fig. 2(a) faster (2.2 s) than the time for the path in Fig. 3(a) (2.7 s). The intuitive reason for the faster motion is that pulling the workpiece in during the motion results in less inertia and allows the motors to move the system faster. With five B-spline control points, the parameter s in the examples lies in the interval $s\in[0,\ 2]$ as shown on the horizontal axis of Fig. 2(b).

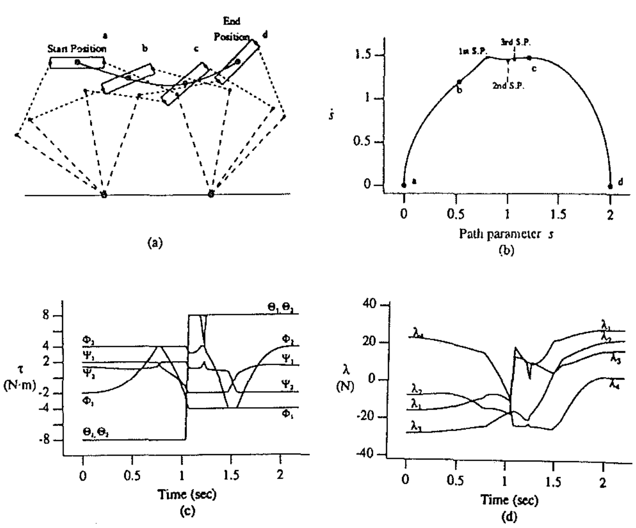

Fig. 2 (a) A fast path, (b) the time-optimal trajectory with three switching points indicated, (c) control torques, (d) internal forces

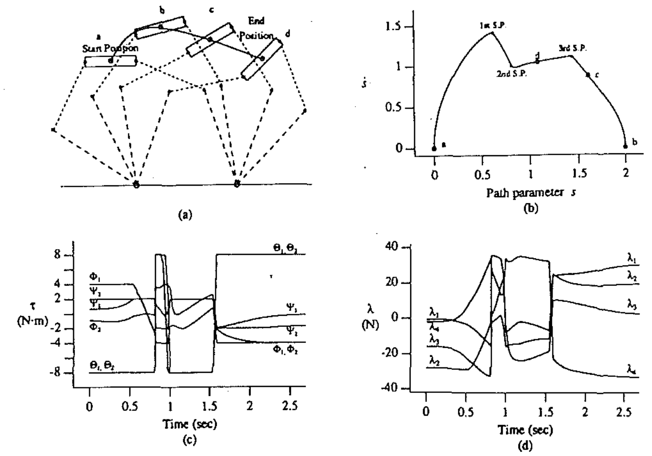

Fig. 3 (*a*) A slower path, (*b*) the time-optimal trajectory with three switching points indicated, (*c*) control torques, (*d*) internal forces

The detailed equations of motion for the system in Fig. 1 are derived in the Appendix. The mass properties and link lengths of each robot arm and the workpiece are listed in Table 1. The distance between the two base joints is 0.4 meter. We assume that there is no friction, and that gravity is zero. These assumptions could simulate a manipulator's work environment in space. The bounds for joint torques are listed in Table 2. Note that the maximum values and the minimum values do not have to be symmetric, nor do they have to be constant throughout the motion.

Case 1: A Fast Path. Because the path is defined using B-splines, it is easy to vary its shape to examine the effect on the computed minimum path traversal time. The total time required for the path in Fig. 2(*a*) was found to be 2.197 seconds, and three switching points are produced, as shown in the phase plane trajectory in Fig. 2(*b*), at times 1.058, 1.197, and 1.238 seconds. All of these switchings occur between positions *b* and *c* of the workpiece shown in 2(*a*). Although one might expect erratic behavior from the joint actuators during these switchings from maximum acceleration to deceleration and vice-versa, and actual torques in 2(*c*) are reasonably well-behaved. Note that, as predicted in the last section, at least 4 ($m+p+1-n=4+6+1-7$) torques are saturated at each instant. No constraints are set on internal forces (or Lagrange multipliers) shown in 2(*d*). The forces acting at the joints of the workpiece are consistent with the time-optimal motion. For instance, λ_2 is the vertical force on the left end of the workpiece and λ_4 is the vertical force on the right end. At the beginning of the motion the large λ_4 causes the twisting motion of the workpiece which results in its motion inwards. The maximum value of λ_2, 28.8 Newtons, occurs at the final position.

Case 2: A Slower Path. A slower path is shown in Fig. 3(*a*). The traversal time was found to be 2.696 seconds, which is 23 percent longer than that required for the previous path. There are three switching points clearly shown in Fig. 3(*b*).

Case 3: Constraints on Internal Forces. The path used here, as well as in the following cases, is the same path used in case 1. In the last two examples, the internal forces were not bounded. In many situations, it may be desirable to reduce forces on the workpiece. In this example, bounds on the internal forces are set at ± 16 Newtons. All that is required to incorporate this bound in the problem is to add it as a constraint for the Simplex algorithm. Note that fewer joint torques are saturated when the internal forces are saturated, see Fig. 4. The sum of saturated torques and saturated internal forces is at least 4, the difference between the number of unknowns and the number of equations of the form (17). The total time required was 2.527 seconds.

Table 1 Link length and mass properties for the robot system

Link	K_1	L_1	K_2	L_2	H
mass (kg)	20	10	20	10	80
length (m)	0.4	0.3	0.4	0.3	0.2

Table 2 Joint torques limits for the robot system

Torque	Θ_1	Φ_1	Ψ_1	Θ_2	Φ_2	Ψ_2
upper bound (N·m)	8	4	2	8	4	2
lower bound (N·m)	−8	−4	−2	−8	−4	−2

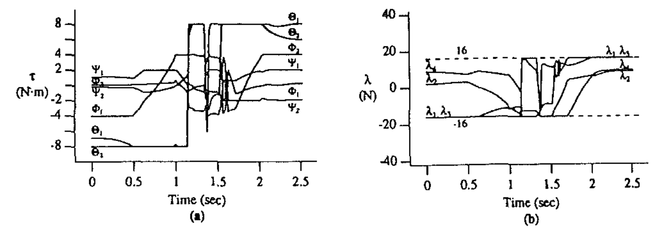

Fig. 4 (*a*) The control torques, (*b*) the internal forces, for motion with constraints on internal forces

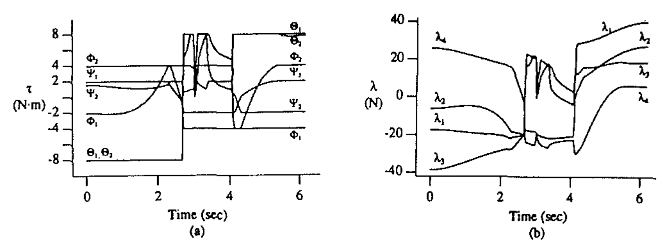

Fig. 5 (*a*) The joint torques, (*b*) the internal forces, for motion with a heavy workpiece

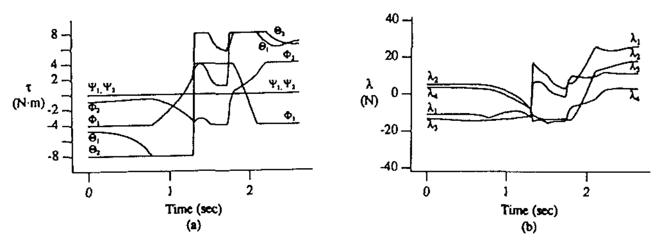

Fig. 6 (*a*) The joint torques, (*b*) the internal forces, for motion with two disabled torques

Case 4: Heavy Workpiece. The weight of the workpiece is increased ten times. The time required for the motion was found to be 6.193 seconds, which, as expected, is much longer than that in case 1. The internal forces shown in Fig. 5, which were not constrained, also increased because of this increase in mass.

Case 5: Two Disabled Actuators. This robot system has three degrees of freedom, so a specified motion can be achieved with any three active motors. In this case, two torques, Ψ_1 and Ψ_2, are disabled. The torque history and internal forces are shown in Fig. 6; the total time was 2.643 seconds.

A summary of the results of all the cases is shown in Table 3. Note that the path traversal time increases for any limitation on either joint torques or internal forces. Also, changing the mass of the workpiece has a significant effect on the motion time.

5 Conclusions

An algorithm has been presented which computes time-optimal trajectories for robot systems with more actuators than degrees of freedom. This is a typical situation for many closed chained systems, including that formed by humans working together on an assembly task. The path taken by the system must be specified, and the algorithm uses a linear programming minimization to resolve the actuator redundancy at each instant.

Examples are given for two planar arms holding a common workpiece. It is shown that arbitrary bounds on the internal forces of interaction on the workpiece may easily be imposed, but this may cause an increase in the path traversal time. The motions found using this algorithm establish a performance limit on cooperating robot systems, and can be used to guide the analysis and design of such systems.

Acknowledgments

The support of the National Science Foundation, grants MSM-8720580 and MSS-9006667, is gratefully acknowledged.

APPENDIX

Let the two robots in Fig. 1 be denoted Robot 1 and Robot 2. The joints of Robot 1 are defined by the position vectors $\mathbf{o}_1$, $\mathbf{a}_1$, and $\mathbf{b}_1$, similarly the joints of Robot 2 are defined by $\mathbf{o}_2$, $\mathbf{a}_2$, and $\mathbf{b}_2$. The rotation angles at each of these joints are respectively denoted as θ_i, ϕ_i, and ψ_i, for $i=1, 2$. The lengths of the first two links of each robot are $K_i = |\mathbf{a}_i - \mathbf{o}_i|$ and $L_i = |\mathbf{b}_i - \mathbf{a}_i|$ for $i=1, 2$. The moving body is the rigid link which connects the end joints $\mathbf{b}_1$ and $\mathbf{b}_2$; its length is H, and its rotation angle is α. The distance between the base joints $\mathbf{o}_1$ and $\mathbf{o}_2$ is D. For convenience, we assume that each link is uniform so that its center of mass lies halfway between the joints it contains.

The dynamics equation of this robot system have the form

$$M\ddot{q} + h(q, \dot{q}) = B\tau + C^T\lambda \tag{23}$$

where $q = \{x, y, \alpha, \theta_1, \phi_1, \theta_2, \phi_2\}^T$ is composed of coordinates of the workpiece and joint angles used to describe the configuration of the robot system, $\tau = \{\Theta_1, \Phi_1, \Psi_1, \Theta_2, \Phi_2, \Psi_2\}^T$ are torques at each joint, and $\lambda = \{\lambda_1, \lambda_2, \lambda_3, \lambda_4\}^T$ are Lagrange multipliers which are equivalent to the internal forces between the robot arms and the workpiece. The 7×7 system mass matrix is

$$M = \begin{bmatrix} M_0 & 0 & 0 \\ 0 & M_1 & 0 \\ 0 & 0 & M_2 \end{bmatrix}, \tag{24}$$

with

$$M_0 = \begin{bmatrix} m^H & 0 & 0 \\ 0 & m^H & 0 \\ 0 & 0 & I^H \end{bmatrix}, \tag{25}$$

$$\mathrm{M}_i = \begin{bmatrix} I^K + I^L + m^K\left(\frac{K}{2}\right)^2 + m^L\left(\frac{L}{2}\right)^2 + m^L K^2 + m^L LK\cos\phi & I^L + m^L\left(\frac{L}{2}\right)^2 + \frac{1}{2}m^L LK\cos\phi \\ I^L + m^L\left(\frac{L}{2}\right)^2 + \frac{1}{2}m^L LK\cos\phi & I^L + m^L\left(\frac{L}{2}\right)^2 \end{bmatrix} \quad i=1, 2. \tag{26}$$

Table 3 Results for five different cases

Case	Description	Time (s)
1	Fastest path found; no constraints on λ.	2.197
2	Slower path; no constraints on λ.	2.696
3	Same path as in 1; constraints are set on λ.	2.527
4	Same path as in 1; weight of workpiece increased 10 times.	6.193
5	Same path as in 1; torques Ψ_1 and Ψ_2 disabled.	2.643

where m stands for mass, I for inertia, and the superscripts K, L refer to the corresponding links with these lengths. Also note that subscripts for K_i, L_i, ϕ_i, etc. in M_i were dropped for clarity.

The 7-vector h which comes from Coriolis and gravitational forces can be written as

$$h = \begin{Bmatrix} h_0 \\ h_1 \\ h_2 \end{Bmatrix}, \tag{27}$$

with

$$h_0 = \begin{Bmatrix} 0 \\ m^H g \\ 0 \end{Bmatrix}, \tag{28}$$

$$h_i = \begin{Bmatrix} -\frac{1}{2}(2\dot{\theta} + \dot{\phi})\dot{\phi} m^L LK\sin\phi + \frac{1}{2}(m^K + 2m^L)gK\cos\theta + m^L g\left(\frac{L}{2}\right)\cos(\theta+\phi) \\ \frac{1}{2}\dot{\theta}^2 m^L LK\sin\phi + m^L g\left(\frac{L}{2}\right)\cos(\theta+\phi) \end{Bmatrix} \tag{29}$$

where g is the acceleration due to gravity. The subscript notation for h_1 and h_2 here were dropped again for clarity.

In Eq. (23), the term $B\tau$ represents the generalized forces that are not obtained from the potential energy in the Lagrangian function. Recall that the elements of B are found by examining the virtual work (Greenwood, 1990) of the actuator torques acting on each independent subsystem. The 7×6 matrix B is

$$B = \begin{bmatrix} 0 & 0 & 0 & 0 & 0 & 0 \\ 0 & 0 & 0 & 0 & 0 & 0 \\ 0 & 0 & 1 & 0 & 0 & 1 \\ 1 & 0 & -1 & 0 & 0 & 0 \\ 0 & 1 & -1 & 0 & 0 & 0 \\ 0 & 0 & 0 & 1 & 0 & -1 \\ 0 & 0 & 0 & 0 & 1 & -1 \end{bmatrix}. \tag{30}$$

The 7×4 matrix C^T is obtained from the holonomic constraints of this robot system, which are the closure equations

$$K_1\cos\theta_1 + L_1\cos(\theta_1+\phi_1) + \frac{1}{2}H\cos\alpha - x - \frac{1}{2}D = 0$$

$$K_1\sin\theta_1 + L_1\sin(\theta_1+\phi_1) + \frac{1}{2}H\sin\alpha - y = 0$$

$$K_2 \cos\theta_2 + L_2 \cos(\theta_2+\phi_2) + \frac{1}{2} H \cos\alpha - x + \frac{1}{2} D = 0$$

$$K_2 \sin\theta_2 + L_2 \sin(\theta_2+\phi_2) + \frac{1}{2} H \sin\alpha - y = 0 \tag{31}$$

Differentiating Eq. (31) with respect to time, we obtain

$$C\dot{q} = 0, \tag{32}$$

where

$$[C] = \begin{bmatrix} A_1^T & J_1 & 0 \\ A_2^T & 0 & J_2 \end{bmatrix} \tag{33}$$

with

$$[A_i] = \begin{bmatrix} -1 & 0 \\ 0 & -1 \\ -\frac{1}{2}\sigma H \sin\alpha & \frac{1}{2}\sigma H \cos\alpha \end{bmatrix}, \quad (i=1,\, 2), \tag{34}$$

$$[J_i]^T = \begin{bmatrix} -K_i \sin\theta_i - L_i \sin(\theta_i+\phi_i) & K_i \cos\theta_i + L_i \cos(\theta_i+\phi_i) \\ -L_i \sin(\theta_i+\phi_i) & L_i \cos(\theta_i+\phi_i) \end{bmatrix}, \quad (i=1,\, 2), \tag{35}$$

where σ equals 1 for Robot 1, and -1 for Robot 2.

References

Bobrow, J. E., 1988, "Optimal Robot Path Planning Using the Minimum-Time Criterion," *IEEE Journal of Robotics and Automation*, Vol. 4, No. 4, pp. 443–450.

Bobrow, J. E., Dubowsky, S., and Gibson, J. S., 1985, "Time-Optimal Control of Robotic Manipulators Along Specified Paths," *International Journal of Robotics Research*, Vol. 4, No. 3, pp. 3–17.

Chen, Y., and Desrochers, A. A., 1988, "Time-Optimal Control of Two-Degree of Freedom Robot Arms," *Proc. IEEE Robotics and Automation Conference*, pp. 1210–1215.

Gilbert, E. G., and Johnson, D. W., 1985, "Distance Functions and Their Applications to Robot Path Planning in the Presence of Obstacles," *IEEE Journal of Robotics and Automation*, Vol. 1, No. 1, pp. 21–30.

Greenwood, D. T., 1988, *Principles of Dynamics*, Prentice Hall.

Kahn, M. E., and Roth, B., 1971, "The Near-Minimum Time Control of Open Loop Articulated Kinematic Chains," ASME Journal of Dynamic Systems, Measurement, and Control, Vol. 93, No. 3, pp. 164–171.

Kreutz, K., and Lokshin, A., 1988, "Load Balancing and Closed Chain Multiple Arm Control," *Proc. American Control Conference*, pp. 2148–2155.

McCarthy, J. M., and Bobrow, J. E., 1992, "The Number of Saturated Actuators and Constraint Forces During a Time-Optimal Movement of a General Robotic System," *IEEE Transactions on Robotics and Automation*, Vol. 8, No. 3, pp. 407–409.

McClamroch, N. H., and Huang, H. P., 1988, "Time-Optimal Control for a Robotic Contour Following Problem," *IEEE Journal of Robotics and Automation*, Vol. 4, No. 2, pp. 140–149.

Meier, E. B., and Bryson, A. E., 1987, "An Efficient Algorithm for Time-Optimal Control of a Two-Link Manipulator," *AIAA Guidance and Control Conference*, pp. 204–212.

Mills, J. K., and Goldenberg, A. A., 1989, "Force and Position Control of Manipulators During Constrained Motion Tasks," *IEEE Journal of Robotics and Automation*, Vol. 5, No. 1, pp. 30–46.

Rajan, V. T., 1985, "Minimum Time Trajectory Planning," *Proc. IEEE Robotics and Automation Conference*, pp. 759–764.

Schumaker, L. L., 1981, *Spline Functions: Basic Theory*, Wiley, New York, NY.

Shiller, Z., and Dubowsky, S., 1988, "Global Time Optimal Motions of Robotic Manipulators in the Presence of Obstacles," *Proc. IEEE Conference on Robotics and Automation*, pp. 370–375.

Shiller, Z., and Dubowsky, S., 1990, "Robust Computation of Path Constrained Time Optimal Motions," *Proc. IEEE Conference on Robotics and Automation*, Cincinnati, Ohio, pp. 144–149.

Shin, K. G., and McKay, N. D., 1985, "Minimum-Time Control of Robotic Manipulators with Geometric Path Constraints," *IEEE Transactions on Automatic Control*, Vol. AC-30, No. 6, pp. 531–541.

Thie, P. R., 1979, *An Introduction to Linear Programming and Game Theory*, Wiley, New York, NY.

Walker, I. D., Freeman, R. A., and Marcus, S. I., 1989, "Internal Object Loading for Multiple Cooperating Robot Manipulators," *Proc. IEEE Robotics and Automation Conference*, Scottsdale, AZ, pp. 606–611.

Zheng, Y. F., and Luh, J. Y. S., 1988, "Optimal Load Distribution for Two Industrial Robots Handling a Single Object," *Proc. of the IEEE Int. Conference on Robotics and Automation*, Philadelphia, PA, pp. 344–349.